IL NUOVO CIMENTO **38 C** (2015) 140
DOI 10.1393/ncc/i2015-15140-0

COLLOQUIA: LaThuile15

# Electroweak Physics (diboson production) measurements with ATLAS

K. BACHAS on behalf of the ATLAS COLLABORATION

*Aristotle University of Thessaloniki - Nuclear and Particle Physics Laboratory*
*54124 University Campus, Thessaloniki, Greece*

received 2 October 2015

**Summary.** — This paper is intended to give an overview of the ATLAS results on the production cross sections of gauge boson pairs using data from $pp$ collisions at $\sqrt{s} = 7\,\text{TeV}$ for $W\gamma, Z\gamma, W^{\pm}W^{\mp}, ZZ, W^{\pm}Z$ and $WV$, where $V = W^{\pm}$ or $Z$ decaying hadronically and $\sqrt{s} = 8\,\text{TeV}$ for $ZZ, W^{\pm}W^{\mp}, W^{\pm}Z$ and $W^{\pm}W^{\pm}$ at the LHC at CERN. The cross sections are found to be in agreement with the expectations from the Standard Model within the estimated uncertainties. The production cross section measurements also allow for studies of anomalous triple and quartic gauge couplings for which 95% confidence limits are set.

PACS 14.70.-e – Gauge bosons.

## 1. – Introduction

Measurements of vector boson pair production provide excellent tests of the electroweak sector of the Standard Model (SM). In the SM, triple gauge couplings (TGC) at tree level are predicted only when there are charged bosons involved, while vertices with all bosons neutral are forbidden. The TGC vertex is completely fixed by the electroweak gauge structure and so a precise measurement of this vertex, through the analysis of diboson production, is essential to test the high energy behavior of electroweak interactions and to probe for possible new physics in the bosonic sector. The non-Abelian gauge nature of the SM predicts, in addition to the TGCs, quartic gauge boson couplings (QGC). The strength of the couplings is set by the universal gauge couplings of the $SU(2)$ local gauge symmetry. Any deviation from gauge constraints can cause a significant enhancement in the production cross section at high diboson invariant mass due to anomalous triple and quartic gauge boson couplings (aTGC and aQGC).

This note presents measurements of the diboson production cross sections in proton-proton collisions and limits on aTGC and aQGC with the ATLAS experiment [1]. The following diboson pair final states were investigated: $W\gamma, Z\gamma, W^{\pm}W^{\mp}, ZZ, W^{\pm}Z, WV (V = W^{\pm}, Z$ decaying to jets) and $W^{\pm}W^{\pm}$. A sample of integrated luminosity $L = 4.6\,\text{fb}^{-1}$

© CERN on behalf of the ATLAS Collaboration
Creative Commons Attribution 4.0 License (http://creativecommons.org/licenses/by/4.0)

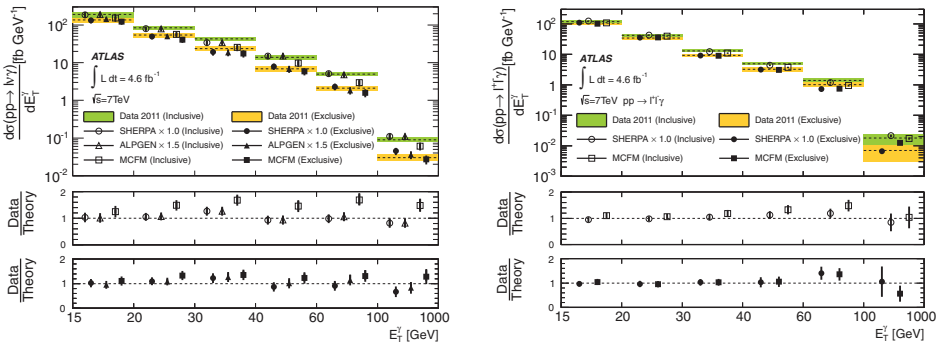


Fig. 1. – Measured $E_T^\gamma$ differential cross sections of the $pp \to \ell\nu\gamma$ (left) and $pp \to \ell\ell\gamma$ (right) processes, using the combined electron and muon measurements by the inclusive ($N_{\rm jet} \geq 0$) and exclusive ($N_{\rm jet} = 0$) fiducial regions. The lower plots show the ratio of the data to the predictions by different generators. The Monte Carlo uncertainties are shown only in the ratio plots [2].

of 2011 data at a center-of-mass energy $\sqrt{s} = 7\,\text{TeV}$ was used for all diboson pair final states except the $W^\pm W^\pm$, while $L = 20.3\,\text{fb}^{-1}$ of 2012 data at $\sqrt{s} = 8\,\text{TeV}$ was used for $ZZ, W^\pm W^\mp$ and $W^\pm W^\pm$. The $W^\pm Z$ measurement used $L = 13\,\text{fb}^{-1}$ of 8 TeV data. All studies used the fully leptonic decay final states with $Z \to \ell\ell$ and $W \to \ell\nu$, where $\ell = e$ or $\mu$, apart from $WV$ where the $V$ is required to decay to jets. The studies of $Z\gamma$ and $ZZ$ channels also considered $\nu\nu\gamma$ and $\ell\ell\nu\nu$ final states, respectively.

## 2. – $W\gamma$ and $Z\gamma$ cross section measurements

The diboson candidate events are selected from the production processes $pp \to \ell\nu\gamma + X$, $pp \to \ell\ell\gamma + X$ and $pp \to \nu\nu\gamma + X$. These final states include the production of $W$ and $Z$ bosons in association with photons from: QED Final State Radiation off the charged leptons, photons radiated from initial-state quarks, photons from the fragmentation of secondary quarks and gluons, and photons radiated by $W$ bosons [2].

Two sets of cross section measurements are performed, namely the inclusive and exclusive, depending on the number of jets in the final state. The inclusive cross section measurement refers to production with no restriction on the number of jets produced. The exclusive measurement refers to events where no central jets with transverse energy $E_T > 30\,\text{GeV}$ are produced. Jets are reconstructed from energy observed in the calorimeter cells using the anti-$k_t$ jet clustering algorithm [3].

The dominating background processes are $Z$+jets, $W$+jets and $\gamma$+jets but there are also contributions from $t\bar{t}$ and $WW$. The systematic uncertainties on the cross sections are dominated by effects coming from the photon identification, background subtraction and jet energy scale uncertainties.

In fig. 1 the measured $E_T^\gamma$ differential cross sections for $pp \to W\gamma \to \ell\nu\gamma$ (left) and $pp \to Z\gamma \to \ell\ell\gamma$ (right) are shown for both the inclusive and exclusive measurements. It is evident that the Alpgen and Sherpa generators describe the $W\gamma$ and $Z\gamma$ distributions in data quite well for both topologies. The inclusive $W\gamma$ measurement is underestimated by the MCFM generator. This is attributed to missing higher-order QCD contributions beyond the available NLO prediction. On the other hand, for $Z\gamma$ the agreement is quite good.

TABLE I. – *Summary of fiducial production cross section of $W\gamma$, $Z\gamma$ channels and comparison with theoretical calculations at LO,NLO and NNLO.*

| | LO (fb) | NLO (fb) | NNLO (fb) | Measurement (fb) |
|---|---|---|---|---|
| $\sigma_{Z\gamma\to\ell\ell\gamma}$ | 850.7 ± 0.2 | 1226.2 ± 0.4 | 1305 ± 3 | 1310 ± 20(stat) ± 110(syst) ± 50(lumi) |
| $\sigma_{W\gamma\to\ell\nu\gamma}$ | 906.3 ± 0.3 | 2065.2 ± 0.9 | 2456 ± 6 | 2770 ± 30(stat) ± 330(syst) ± 140(lumi) |

A new fully differential computation of radiative corrections at next-to-next-to-leading order (NNLO) in QCD perturbation theory has become available since these analyses were published and can be found in refs. [4,5]. Corrections are sizeable for the $W\gamma$ case, which can reach up to $\sim 20\%$ with respect to NLO calculations. Smaller corrections for $Z\gamma$ are reported. Table I summarizes the results for each case, where it is evident that the measurement agrees better with the updated SM predictions at NNLO.

## 3. – $WW$ cross section measurement

The $WW \to \ell\nu\ell\nu$ signal is measured in final states with two oppositely charged isolated leptons and large missing transverse energy [6, 7]. Candidate $WW$ events are required to have no jets reconstructed in the final state because the background dominates at higher jet multiplicities as can be seen in the left plot of fig. 2, where the reconstructed jet multiplicity is shown for data and Monte Carlo simulation(MC).

Processes that can mimic the $\ell\ell$+$E_T^{miss}$ signal with no reconstructed jets are top-quark production, when then event contains jets falling outside the acceptance and thus passing the jet veto requirement, $W$+jets when a jet fakes a lepton (fake lepton), Drell-Yan with mismeasured jets and diboson channels.

The measured total production cross section at $\sqrt{s} = 7\,\text{TeV}$ is $51.9 \pm 2.0(\text{stat.}) \pm 3.9(\text{syst.}) \pm 2.0(\text{lumi.})\,\text{pb}$ while the theoretical prediction gives $44.7^{+2.1}_{-1.9}\,\text{pb}$. At $\sqrt{s} = 8\,\text{TeV}$ the measured total cross section is $71.4 \pm 1.2(\text{stat.})^{+5.0}_{-4.4}(\text{syst.})^{+2.2}_{-2.1}(\text{lumi.})$ while the SM prediction is $58.7^{+3.0}_{-2.7}\,\text{pb}$. The driving uncertainty on the measurement is the systematic uncertainties associated with the jet veto requirement and the estimation of backgrounds from "fake" leptons using data driven methods.

The right plot of fig. 2 summarizes the results of the $WW$ analysis. The cross sections measured in the individual channels as well as the combined cross section are shown and compared to the SM prediction, which is obtained using the CT10 PDF set. As can be seen, the individual channels are compatible within their uncertainties, however all measurements lie above the SM prediction. The statistical significance of the observed enhancement is $2.1\,\sigma$ for the $e\mu$ channel, $1.1\,\sigma$ for the $ee$ channel and $1.3\,\sigma$ for the $\mu\mu$ topology.

Since this result was presented there has been an effort to improve the theoretical calculations by computing NNLO corrections which can account for $\sim 10\%$ of the difference, while other calculations based on resummation of large logarithms that arise from a jet-veto condition, provide further corrections. These results are reported in refs. [8-10].

## 4. – $WZ$ and $ZZ$ production cross section measurements

The analyses of $W^{\pm}Z$ boson pairs is performed in $3\ell\nu$ final states while the $Z$ boson pair production is performed in the $4\ell$ and $2\ell2\nu$ final states [11-14]. In the $ZZ$ to $2\ell2\nu$ topology the analysis is performed only with the $\sqrt{s} = 7\,\text{TeV}$ data sample.

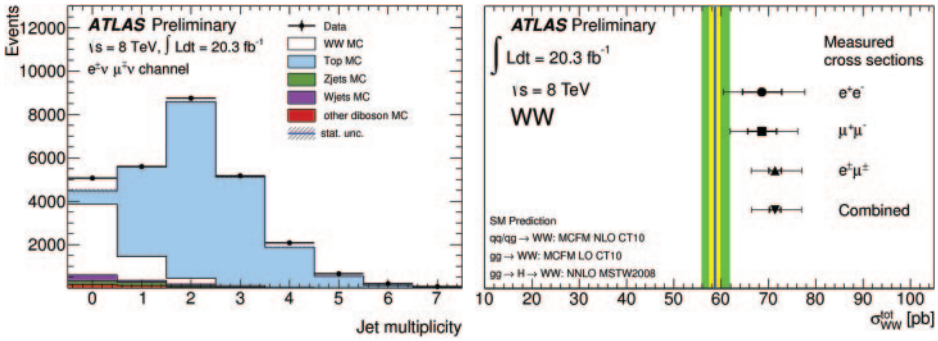


Fig. 2. – Left: Jet multiplicity distribution for $e\mu$ events. The points represent data and the stacked histograms are the MC predictions. Only statistical uncertainties are shown. Right: Comparison between predicted $WW$ production cross section at $\sqrt{s} = 8\,\text{TeV}$ using CT10 PDF and the measured cross section in $ee, \mu\mu, e\mu$ and combined channels. The yellow and green shaded bands represent the PDF and total theoretical uncertainties respectively. The filled symbols show the measured total cross section with the statistical and total uncertainty

The main sources of background to the $W^{\pm}Z \to 3\ell\nu$ final state come from $Z$+jets and $t\bar{t}$ events, where the two leptons from the vector boson decays are accompanied by a jet which is misidentified as a lepton. These backgrounds are estimated from data-driven techniques. There is also a contribution from $ZZ$ events in which one of the leptons falls outside the acceptance of the detector and thus creates $E_T^{miss}$. This source is estimated from MC.

The $4\ell$ final state is a very clean signature with small background contributions. These mainly come from $Z$+jets and $t\bar{t}$ processes where the jets are misidentified as leptons and are estimated with data-driven methods. The background is more significant in the $2\ell 2\nu$ final state and is a mixture of diboson, $t\bar{t}$ and Drell-Yan events.

The dominant uncertainty in the $WZ$ cross section measurement is the systematic uncertainty in the data driven background estimation. The $ZZ$ measurement is dominated by statistical uncertainties while the systematics are dominated by lepton identification and resolution.

The results on the total production cross-section for both measurements at 7 and 8 TeV are presented in fig. 3 and compared to SM predictions. Overall good agreement with the predictions from the SM is found.

## 5. – $WW + WZ$ production cross section measurement

The production of a $W$ boson decaying to $e\nu$ or $\mu\nu$ in association with a $W$ or $Z$ boson decaying to two jets is studied using the data sample at $\sqrt{s} = 7\,\text{TeV}$ [19].

Candidate $WV \to \ell\nu jj$ events are required to contain exactly one lepton, large missing transverse momentum and exactly two jets. The selected events are accepted if they pass a set of kinematic cuts chosen to enhance the signal-to-background ratio. The $WW+WZ$ signal yield is obtained by performing a binned maximum-likelihood fit to the dijet mass ($m_{jj}$) distribution using templates based on MC. The fit is performed on events in an $m_{jj}$ range much larger than the range where the signal peaks, allowing the nearly signal-free dijet regions to constrain the rate of the $W$ + jets events, which are the largest background.

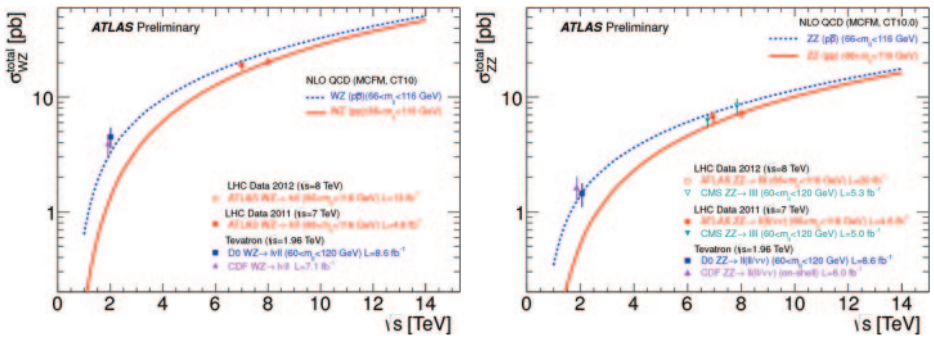


Fig. 3. – Measurements and theoretical predictions of the total $WZ$ (left) and $ZZ$ (right) production cross section as a function of center-of-mass energy $\sqrt{s}$. Experimental measurements from CDF [15, 16] and D0 [17] in $p\bar{p}$ collisions at the Tevatron at $\sqrt{s} = 1.96\,\text{TeV}$ and experimental measurements from ATLAS in $pp$ collisions at the LHC at $\sqrt{s} = 7\,\text{TeV}$ and $\sqrt{s} = 8\,\text{TeV}$ are shown. The blue dashed line shows the theoretical prediction for the $WZ/ZZ$ production cross section in $p\bar{p}$ collisions. The solid red line shows the theoretical prediction for the $WZ/ZZ$ production cross section in $pp$ collisions. For the $ZZ$ channel, the CMS [18] results are also shown.

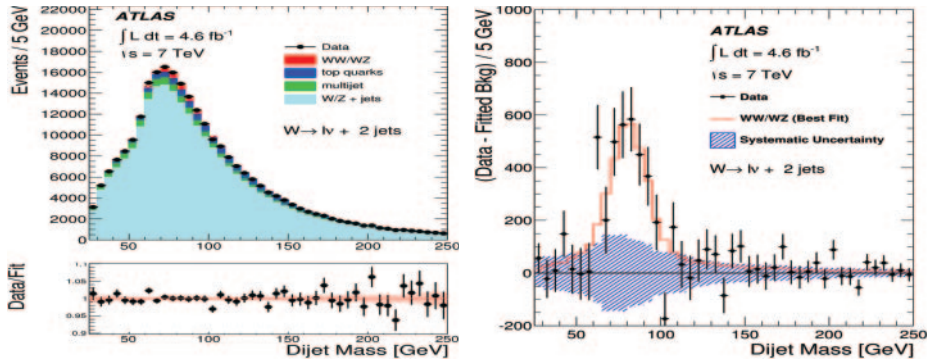


Fig. 4. – Left: dijet invariant mass distributions after the likelihood fit for the combined electron and muon topology final states. The error bars represent statistical uncertainties, and the stacked histograms are the signal and background contributions. The lower panel displays the ratio between the data and the total fit result, including both signal and backgrounds. The hatched band shows the systematic uncertainty on the fitted signal plus background. Right: dijet mass distribution of the background-subtracted data for the sum of the electron and muon channels. The error bars represent the statistical error on the data.

Backgrounds, apart from the $W$ + jets process, are the multi-jet, top and diboson events. Multi-jet background, like the dominant $W$ + jets, is estimated with data-driven techniques, while the other two are estimated from MC.

The left plot of fig. 4 shows the dijet invariant mass distribution after the likelihood fit for the combined electron and muon final states. The normalisations and shapes of the histograms are obtained from the best fit to the data, after being allowed to vary within their systematic uncertainties. Good overall agreement is seen between the data and the total fit result. The dijet mass distribution of the background-subtracted data for the sum of the electron and muon channels is shown on the right plot.

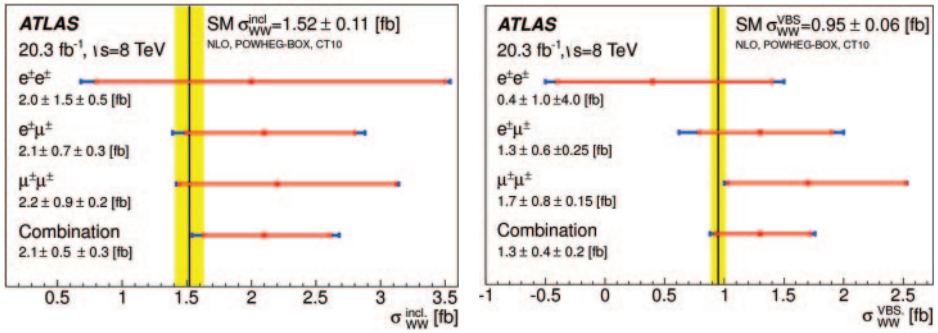


Fig. 5. – The measured fiducial cross sections for the inclusive region (left) and the VBS region (right) compared to the predicted SM fiducial cross section. The inner red error band represents the statistical error and the end of the blue band defines the total error on each measurement.

The $W/Z \to jj$ resonance is observed with a $3.4\,\sigma$ significance while the measured total production cross section is $68 \pm 7(\text{stat.}) \pm 19(\text{syst.})$, in good agreement with the expectation from the SM which is $61.1 \pm 2.2$.

## 6. – Same charge $WW$ production cross section measurement

The scattering of $W$ bosons accompanied by 2 jets (Vector Boson Scattering - VBS), is a great tool to probe the nature of electroweak symmetry breaking. Assuming there were no SM Higgs boson, the VBS amplitude would increase as a function of the center-of-mass energy and would violate unitarity at energies around 1 TeV. The recent discovery of the Higgs boson explains the mechanism that governs the Electroweak Symmetry Breaking and unitarizes the VBS process. However many physics scenarios predict enhancements in the VBS cross section above 1 TeV either from additional resonances or if the observed SM-like Higgs boson only partially unitarizes the VBS. Additionally, there is no previous evidence for a process involving a $VVVV$ vertex [20].

The same charge $WW + 2$ jets ($ssWWjj$) analysis proceeds through the leptonic final state to electrons and/or muons. Two types of processes give rise to $ssWWjj$ final states. The first process, which includes VBS contributions, involves exclusively weak interactions. The second process involves both strong and electroweak interactions and is refered to as strong production.

The main backgrounds in this measurement are the $WZ$+2 jets and the $W\gamma$+2 jets. To separate between strong and pure electroweak production a requirement on the dijet mass above 500 GeV is applied. To enhance the VBS contribution, an additional requirement on the rapidity difference between the two jets is applied as $|\Delta y_{jj}| > 2.4$.

Results from the $ssWWjj$ analysis are summarized in fig. 5 where the measured fiducial cross sections are shown for the inclusive region (left) and the VBS region (right) compared to the predicted SM cross sections. The combined significance over background only hypothesis is $4.5\,\sigma$ in the inclusive and $3.6\,\sigma$ in the VBS region.

## 7. – Triple and quartic gauge couplings measurements

The non-Abelian nature of the electroweak sector of the SM predicts the self-interaction of gauge bosons in the form of triple and quartic couplings. Searches for

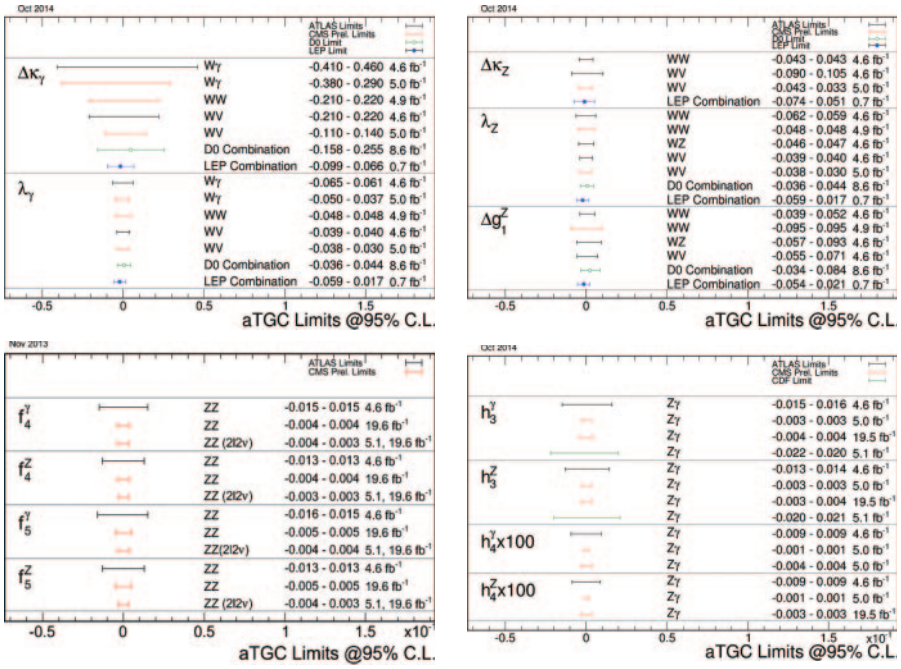


Fig. 6. – Top plots: Comparison of results from ATLAS, CMS, CDF, D0 and LEP experiments on limits on charged anomalous triple gauge couplings at 95% CL. Bottom plots: Comparison of results from ATLAS, CMS, CDF, D0 and LEP experiments on limits on neutral anomalous triple gauge couplings at 95% CL [21].

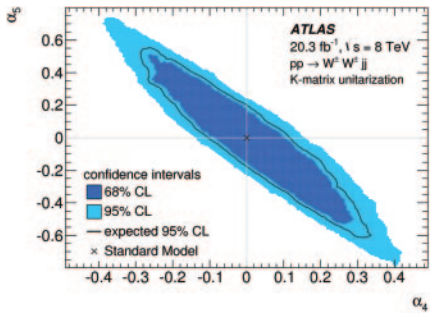


Fig. 7. – Limits on $(\alpha_4, \alpha_5)$. Points outside of the solid light ellipse are excluded by the data at 95% confidence level (CL). Points outside the inner dark ellipse are excluded at the 68% confidence level. The expected exclusion is given by the solid line.

deviations from the SM can be parametrized in terms of anomalous triple and quartic gauge couplings (aTGC and aQGC) using an effective lagrangian.

In fig. 6(a) summary of the limits set on the different aTGC parameters is shown along with comparisons to other experiments. No deviations from the expected SM values is observed in any channel.

The measurement of the VBS production cross section in the same charge $WW+2$jets channel allows for limits to be set on anomalous quartic couplings. Deviations from

the predictions of the SM are parametrized in terms of parameters $\alpha_4$ and $\alpha_5$ [20]. Figure 7 shows the limits on the $(\alpha_4, \alpha_5)$ space. The observed 1-dimensional limit on $\alpha_4$ is $[-0.139, 0.157]$ and $[-0.229, 0.244]$ for $\alpha_5$. The expected limits are $[-0.104, 0.116]$ and $[-0.180, 0.199]$ respectively.

## 8. – Conclusions

Measurements of the production cross sections of $W\gamma, Z\gamma, W^{\pm}W^{\mp}, ZZ, W^{\pm}Z, WV$, where $V = W^{\pm}$ or $Z$ decaying to jets, and $W^{\pm}W^{\pm}$ have been performed with the ATLAS detector at center-of-mass energies $\sqrt{s} = 7\,\text{TeV}$ and $8\,\text{TeV}$. The total production cross sections are compatible with the SM expectations within uncertainties. No evidence for new physics is observed from the kinematic distributions of the diboson processes. Limits on anomalous triple and quartic gauge couplings are set in all channels and values of aTGC and aQGC parameters are well within the SM predictions.

* * *

This research has been co-financed by the European Union (European Social Fund ESF) and Greek national funds through the Operational Program Education and Lifelong Learning of the National Strategic Reference Framework (NSRF) - Research Funding Program: Thales. Investing in knowledge society through the European Social Fund.

REFERENCES

[1] ATLAS Collaboration, *JINST*, **3** (2008) S08003.
[2] ATLAS Collaboration, arXiv:1302.1283.
[3] Cacciari M., Salam G. P. and Soyez G., *JHEP*, **04** (2008) 063.
[4] Grazzini M., Kallweit S., Rathlev D. and Torre A., *Phys. Lett. B*, **731** (2014) 204.
[5] Grazzini M., arXiv:1407.1618.
[6] ATLAS Collaboration, arXiv:1210.2979.
[7] ATLAS Collaboration, ATLAS-CONF-2014-033, http://cds.cern.ch/record/1728248.
[8] Gehrmann T. *et al.*, arXiv:1408.5243.
[9] Jaiswal P. and Okui T., arXiv:1407.4537.
[10] Meade P., Ramani H. and Zeng M., arXiv:1407.4481.
[11] ATLAS Collaboration, *Eur. Phys. J. C*, **72** (2012) 2173.
[12] ATLAS Collaboration, ATLAS-CONF-2013-021, http://cds.cern.ch/record/1525557.
[13] ATLAS Collaboration, *JHEP*, **03** (2013) 128.
[14] ATLAS Collaboration, ATLAS-CONF-2013-020, http://cds.cern.ch/record/1460409.
[15] CDF Collaboration, *Phys. Rev. Lett.*, **108** (2012) 101801.
[16] CDF Collaboration, *Phys. Rev. D*, **86** (2012) 031104.
[17] D0 Collaboration, *Phys. Rev. D*, **85** (2012) 112005.
[18] CMS Collaboration, *JHEP*, **1301** (2013) 063.
[19] ATLAS Collaboration, *JHEP*, **01** (2015) 049.
[20] ATLAS Collaboration, *PRL*, **113** (2014) 141803.
[21] http://twiki.cern.ch/twiki/bin/view/CMSPublic/PhysicsResultsSMPaTGC.